Deep Learning-Based Ovitrap Spatial Dynamics Analysis for Arbovirus Vector Monitoring.

Ignacio Sanchez-Gendriz
DCA, LAIS
Federal University of Rio Grande do Norte
RN, Brazil
ignacio.gendriz@lais.huol.ufrn.br

Matheus Diniz
DCA
Federal University of Rio Grande do Norte
RN, Brazil
matheus.diniz.122@ufrn.edu.br

A. D. Doria Neto
DCA
Federal University of Rio Grande do Norte
RN, Brazil
adriao@dca.ufrn.br

Rodrigo Moreira Pedreira
Municipal Health Department
Zoonoses Control Center
RN, Brazil
rodrigompedreira@gmail.com

Ion de Andrade
LAIS
Federal University of Rio Grande do Norte
RN, Brazil
ion.andrade@lais.huol.ufrn.br

R. A. de Medeiros Valentim
LAIS
Federal University of Rio Grande do Norte
RN, Brazil
ricardo.valentim@lais.huol.ufrn.br

***Abstract*—Dengue is a significant global health issue, affecting millions of people annually and imposing substantial socioeconomic burdens. Effective disease control relies on monitoring the population of *Aedes aegypti* mosquitoes, the primary vector of dengue. One surveillance method involves counting the eggs laid by these mosquitoes in spatially distributed ovitraps. This study focuses on the application of computational methods to forecast dengue vector populations. We analyze a four-year (2016-2019) database from 397 ovitraps distributed across Natal, RN-Brazil, with a weekly sampling frequency. Our objective is to develop accurate machine learning (ML) models that can predict the egg density index (EDI) at a fine-grained spatial resolution, aligned with zoonosis interventions. To preprocess the dataset obtained from the ovitraps, we employ spatial smoothing techniques and aggregation. The preprocessed data is then used to train ML models, including recurrent deep learning (DL) models, enabling accurate forecasting of the EDI. This approach shows promise for monitoring and preventing arbovirus outbreaks. Our findings demonstrate the effectiveness of spatial smoothing and aggregation as preprocessing steps for reducing randomness and noise in the dataset. The recurrent DL models exhibit high forecasting accuracy, thereby validating their utility in arbovirus monitoring and prevention efforts.**

***Index Terms*—Machine learning, deep learning, arboviruses forecasting, dengue, ovitraps.**

I. Introduction

A. Aedes aegypti as a vector for several diseases

Aedes aegypti serves as the primary vector for the transmission of several significant diseases, including Dengue, chikungunya, zika virus, and yellow fever [1]. Consequently, methods that enable effective monitoring of Aedes aegypti populations play a crucial role in public health interventions [2]. One such monitoring method involves the use of ovitraps, specialized containers that mimic suitable conditions for mosquito egg deposition [3]. By quantifying the number of Aedes aegypti eggs collected in ovitraps distributed throughout a city, we can obtain a spatio-temporal proxy for vector incidence [4], [5].

B. Potentials of ovitrap data analysis

In previous work our group demonstrated the application of ovitrap for early prediction of dengue incidence in the city of Natal/RN-Brazil [5]. Building upon this foundation, the primary objective of the current study is to forecast vector incidence through the monitoring of ovitraps in Natal. By predicting future values associated with egg density, our aim is to provide public health stakeholders with timely and spatially relevant information for early interventions. In this regard, we evaluate various Machine Learning (ML) models, including Multilayer Perceptron (MLP), Long Short-Term Memory (LSTM), and Gated Recurrent Unit (GRU), for predicting ovitrap data.

C. Structure of manuscript

Regarding the structure of manuscript, Section 2 provides a comprehensive description of the dataset, outlining the preprocessing and data preparation techniques utilized, as well as the ML models employed for prediction. It also details the strategy adopted for training, validation, and testing of the models. In Section 3, we present the results of Exploratory Data Analysis (EDA) conducted on the ovitrap data. We compare the performance of the ML models and showcase their applicability in forecasting spatio-temporal ovitrap data.

Section 4 discusses the findings of the study, comparing and contrasting them with existing literature on the topic. Finally, in Section 5, we present the final conclusions and highlight potential avenues for future research..

II. Material and methods

A. Ovitrap data description

In this study, we analyzed a dataset comprising egg counts for Aedes aegypti mosquitoes, collected during each epidemiological week from 2016 to 2019 in the city of Natal. It is worth noting that, in the field of epidemiology, a year is conventionally divided into 52 epidemiological weeks. Therefore, for the four years under analysis, we have a total of 208 epidemiological weeks. The dataset consists of egg counts obtained from 397 strategically distributed ovitraps throughout the city. Trained personnel conducted manual counts of eggs using microscopes and a hand counter, adhering to established protocols. These counts were reported by the Zoonoses Center of Natal, ensuring accuracy and consistency. The spatial distribution of the ovitraps can be visualized in Figure 1, providing a clear representation of their locations within the city.

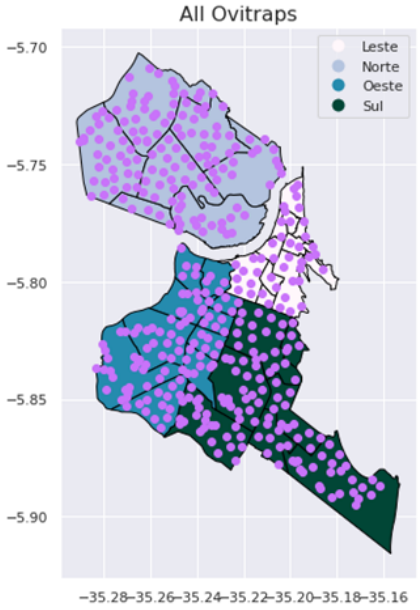

Fig. 1. Spatial distribution of ovitraps in Natal city.

B. Data prepossessing

The analysed dataset encompassed a total of 397 ovitraps, as mentioned in the previous section. However, to ensure data quality and mitigate potential biases, a criterion was applied to remove ovitraps with an average egg count of less than 1. This selection process aimed to exclude ovitraps that were likely to be neglected or exhibited potential biases in egg counts or material collection. Consequently, the final dataset used in this study comprised 297 ovitraps, which will be referred to as the 'cleaned dataset'.

C. Spatial smoothing and aggregation

To optimize the dataset for further analysis, we applied two essential preprocessing techniques: spatial smoothing and aggregation. Subsequently, we provide a detailed explanation of both processes.

Spatial Smoothing: To account for the assumption that neighboring points would exhibit similar conditions for mosquito reproduction, a neighborhood was defined for each ovitrap by considering its five nearest points based on Euclidean spatial distance. For each ovitrap, the mean value computed from its neighborhood was determined. This spatial smoothing process aimed to reduce randomness at local points by replacing the local value with the average value obtained from its vicinity.

Aggregation: In order to establish spatial areas that align with the actual conditions for vector control interventions, a group of four ovitraps was aggregated using the mean average. This aggregation not only computed the mean of the egg counts within the group but also determined a centroid based on the mean of the spatial points considered in each case. This aggregation approach facilitates targeted interventions at precise locations and helps mitigate the impact of outliers and randomness in the analyzed data. The aggregation process, performed through mean averaging, yielded a commonly used indicator known as the Egg Density Index (EDI) [6]. Affetr data aggregation step, we finalize with 67 spatial points (aggregated ovitrap data).

III. Model training and selection

In this study, we employed a set of eight models categorized into three distinct groups for arbovirus forecasting. The first group consisted of traditional feedforward neural networks, while the second and third groups comprised Deep Learning (DL) recurrent neural networks (RNNs). The first group included two Multilayer Perceptron models (MLP1 and MLP2). The second group utilized three Long Short-Term Memory models (LSTM1, LSTM2, and LSTM3). Lastly, the third group incorporated three Gated Recurrent Unit models (GRU1, GRU2, and GRU3). Each model in these groups exhibited unique characteristics in terms of parameters and structural variations. These differences allowed for a comprehensive exploration of various aspects of arbovirus forecasting. It is noteworthy that both MLP models and recurrent neural networks such as LSTM and GRU have been extensively used for forecasting purposes in epidemiology, demonstrating their applicability and effectiveness in similar domains [7], [8].

The selection of these models was based on their ability to capture complex relationships in the data and address the challenges associated with time series prediction. The variations in their architectures provided a diverse set of models to explore different aspects of arbovirus forecasting.

Our training approach involved using a sliding time window (see Fig. 2), where we utilized data from the preceding 4 weeks to predict the data for the subsequent week. This method allowed us to effectively forecast vector incidence one week ahead, providing valuable insights for timely and

accurate prediction of vector monitoring and control efforts. As depicted in Fig. 2, all models were configured with an input of 4 elements and an output of 1 element. Thus, for all the models implemented in this work, we used an input layer with 4 neurons, and an output layer with 1 neuron, employing the Rectified Linear Unit (ReLU) activation function.

To provide a succinct description of the model architecture, we have adopted the format $NI : NH_x : NO$, where NI represents the number of neurons in the input layer, NH_x represents the number of neurons in hidden layer x, and NO represents the number of neurons in the output layer. This format offers a concise overview of the neural network structure by indicating the neuron count for each layer.

In our specific models, we have followed this format to describe the architecture, providing the number of neurons in the input layer, the hidden layers, and the output layer. Additionally, we include detailed information about the type of layers used eachmodel, such as the specific activation functions employed. This comprehensive description enables us to easily identify the dimensions and characteristics of each layer within the neural network, facilitating a clear understanding of its composition and functionality.

In the following paragraphs, we will provide a brief description of the different architectures for each individual model.

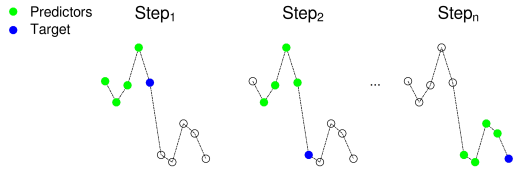

Fig. 2. Approach used for training the models.

1) Group 1: Multilayer Perceptron (MLP) is a type of artificial neural network composed of interconnected layers of neurons. The intermediate layers, known as hidden layers, enable the MLP to learn complex representations of the input data, while the output layer generates the final model's response. We tested two MLP architectures:

MLP1 (4:8:16:1):

- Hidden layer with 8 neurons and activation function: Linear.
- Hidden layer with 16 neurons and activation function: Sigmoid.

MLP2 (4:8:32:1):

- Hidden layer with 8 neurons and activation function: Linear.
- Hidden layer with 32 neurons and activation function: Sigmoid.

2) Group 2: Long Short-Term Memory (LSTM) is a type of recurrent neural network (RNN) specifically designed to address the gradient vanishing problem in long sequences. LSTM cells have a specialized structure that allows them to store and retrieve information over time. We utilized three LSTM architectures:

LSTM1 (4:32:1):

- Hidden layer with 32 LSTM neurons and activation function: Rectified Linear Unit (ReLU).

LSTM2 (4:128:1):

- Hidden layer with 128 LSTM neurons and activation function: Rectified Linear Unit (ReLU).

LSTM3 (4:128:128:1):

- Hidden layer with 128 LSTM neurons and activation function: Rectified Linear Unit (ReLU).
- Hidden layer with 128 LSTM neurons and activation function: Rectified Linear Unit (ReLU).

3) Group 3: Gated Recurrent Unit (GRU) is another type of RNN that also addresses the gradient vanishing problem. GRU has gate mechanisms that control the flow of information, but with a simplified structure compared to LSTM. GRUs have a single memory cell that can be updated, reset, or read from one time step to the next. This compact structure results in fewer parameters and faster training. We employed three GRU architectures:

GRU1 (4:32:1):

- Hidden layer with 32 GRU neurons and activation function: Rectified Linear Unit (ReLU).

GRU2 (4:128:1):

- Hidden layer with 128 GRU neurons and activation function: Rectified Linear Unit (ReLU).

GRU3 (4:128:128:1):

- Hidden layer with 128 GRU neurons and activation function: Rectified Linear Unit (ReLU).
- Hidden layer with 128 GRU neurons and activation function: Rectified Linear Unit (ReLU).

A. Training, validation, and test

For all the models, we utilized a simple hold-out cross-validation approach for training and testing. The dataset was split into 80% (166 weeks) for training (132 weeks) and validation (34 weeks), while the remaining 20% (42 weeks) was reserved for testing. However, to ensure robust estimation of model performance, we implemented a resampling cross-validation technique [9] with 10 repetitions.

In each repetition, we randomly selected 40 ovitraps from the dataset and computed the average time series based on the selected ovitrap data points. The models were then trained on the 132 weeks of training data and evaluated on the remaining 34 weeks of the validation set. Model performance was assessed using the Root Mean Square Error (RMSE) and Mean Absolute Error (MAE) across the 10 repetitions, as these metrics are widely used in the literature to evaluate model performance [10].

Based on the mean RMSE and MAE metrics computed on the 10 repetitions for the validation set, we identified the top two models with the lowest errors for further analysis.

The testing phase consisted of two aspects: testing on the averaged (univariate) mean aggregated time series and testing on the complete aggregated time series, which comprised 67 different data points.

Our primary objective was to train a spatio-temporal model capable of predicting future values for each aggregated ovitrap data point, representing spatial locations over time. This approach enables early identification of areas requiring public health interventions and provides valuable insights into when and where to implement preventive vector management strategies.

By employing this methodology, our aim was to develop robust models that can accurately forecast arbovirus vector populations, facilitating targeted interventions for effective disease control.

IV. Results and Discussion

A. Exploratory Data Analysis (EDA)

Heat maps of the ovitrap data are presented in Fig.3, revealing distinct periods throughout the year that are more favorable for mosquito reproduction, particularly between January and June, while the remaining months are less conducive to mosquito proliferation. This visualization underscores the need to increase warnings, public health actions, and interventions during the rainy periods. Fig.3a displays the raw ovitrap data, which includes certain data points that raised doubts regarding their accuracy in terms of egg counts. Consequently, the original data underwent cleaning procedures as explained in Section II-C. By removing unreliable ovitraps, the spurious patterns observed in the heat map were eliminated, as evidenced by the comparison between Fig.3a and Fig.3b. This visual comparison clearly shows the removal of missing data patterns in Fig.3b that were initially evident in Fig.3a.

Additionally, Fig.3c represents the smoothed ovitrap data. Initially, the dataset was reduced from 397 to 271 ovitraps (Fig.3a to Fig.3b) through the cleaning process. Subsequently, the aggregation step explained in Section II-C further reduced the dataset from 271 to 67 ovitraps, achieving a more concise representation.

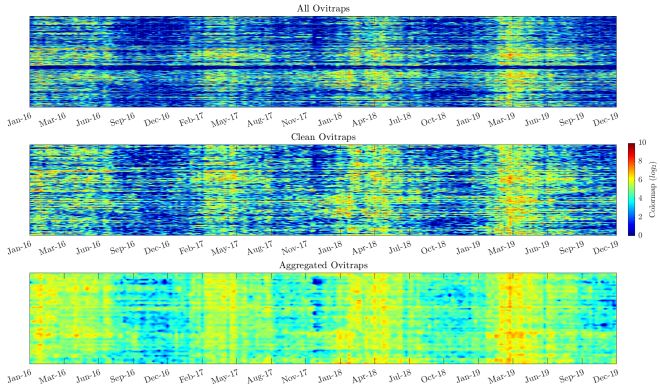

Fig. 3. Heat maps representing the ovitrap data. A $\log_2$ transformation was applied to facilitate data visualization. (a) Raw data containing all ovitraps. (b) Clean data, excluding ovitraps with extreme low values of egg counts. (c) Spatial smoothing ovitrap data.

To gain a better understanding and quantify the relationship between vector incidence and climatic variables, we analyzed the precipitation data for the Natal city. Fig.4 demonstrates a strong correlation between precipitation and the Egg Density Index (EDI). Fig.4a depicts a heat map illustrating the mean monthly values of EDI for the aggregated ovitrap data, while Fig.4b represents the time series of the mean EDI data shown in Fig.4a, alongside the accumulated precipitation time series. Both time series (EDI and precipitation) were normalized within the range of 0 to 1, and smoothed by using a moving average filter, facilitating a visual comparison. Notably, EDI and precipitation exhibit a robust association. A simple inspection of Figure 3a and Figure 3b confirms that periods with high precipitation values align with increased EDI. To quantitatively assess this relationship, we computed the Pearson correlation coefficient, yielding a correlation of r = 0.72 and a p-value of 9.76×10^{-9}, indicating a statistically significant and strong correlation between precipitation and EDI.

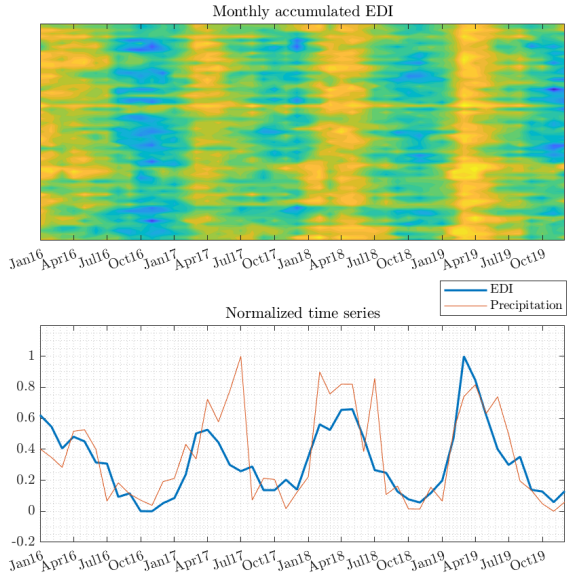

Fig. 4. Relation between EDI and precipitation accumulated monthly in Natal City; a) Heat map of EDI accumulated by monthly values, b) mean EDI accumulated by months and monthly values of accumulated precipitation.

These findings highlight the substantial influence of climatic factors, specifically precipitation, on mosquito populations and the consequential implications for disease transmission. The strong correlation between EDI and precipitation underscores the potential of incorporating meteorological data into arbovirus forecasting models and emphasizes the significance of proactive measures during periods of heightened precipitation.

B. Model validation and performance

The models underwent evaluation based on the mean RMSE and MAE metrics computed on the validation dataset using the resampling approach described in Section III-A. The performance metrics are presented in Table I. The results indicated that the MLP models had poor performance, while the LSTM and GRU models showed superior performance, with similar results between the two groups. Consequently, we selected the simplest model from each group, namely LSTM1 and GRU1, for further analysis.

The selected models, LSTM1 and GRU1, were re-trained using the complete training and validation dataset, which encompassed 166 weeks of data. This training was conducted on the average (univariate) time series obtained by averaging data from individual ovitraps illustrated in the heat map of Fig.4a. This extended training provided the models with the opportunity to learn from a larger and more diverse dataset, enabling them to capture a wider range of temporal patterns and improve their predictive capabilities. By leveraging this expanded dataset, our aim was to enhance the models' performance and reliability in accurately forecasting arbovirus vector populations. The inclusion of additional data allowed the models to extract valuable insights and capture intricate relationships, ultimately leading to more robust and accurate predictions.

Model	MAE	RMSE
MLP1	24.95	29.39
MLP2	19.21	24.14
LSTM1	6.64	9.83
LSTM2	6.69	9.44
LSTM3	6.61	9.42
GRU1	6.58	9.95
GRU2	6.57	9.28
GRU3	6.75	9.23

TABLE I
MODEL EVALUATION METRICS

Fig.5 illustrates the time series of the mean aggregated EDI, showcasing the true values alongside the predictions from the selected models. The models closely align with the true values, validating their performance.

The LSTM1 and GRU1 models were utilized to predict the values for each individual aggregated ovitrap, despite being trained on the mean of all spatial points. Fig.6 presents heatmaps that compare the true values with the predicted values from each model. Upon visual examination of the heatmaps, it is evident that both models accurately capture the true trends of the individual spatial data points.

The LSTM1 model yielded MAE and RMSE values of 7.4 and 9.7, respectively, on the mean EDI (Fig.5), while the GRU1 model achieved MAE and RMSE values of 7.7 and 10.5, respectively. These results align closely with the validation errors reported in Table I.

Furthermore, we assessed the performance of LSTM1 and GRU1 models in predicting individual values for each ovitrap. When evaluating the MAE and RMSE on individual ovitraps (Fig.6), LSTM1 achieved scores of 13.4 and 18.1, while GRU1 yielded scores of 14.6 and 19.8, respectively.

It is important to acknowledge that the performance of the models declined when predicting individual ovitrap values. This decrease in performance can be attributed to the models being trained on the mean average, which fails to capture the unique dynamics exhibited by individual ovitraps. It is

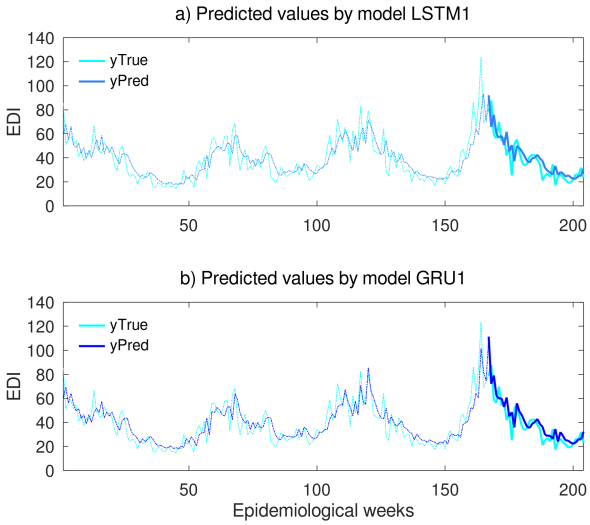

Fig. 5. Performance comparison of models based on the EDI time series. (a) Comparison of the GRU3 model's performance. (b) Comparison of the LSTM4 model's performance

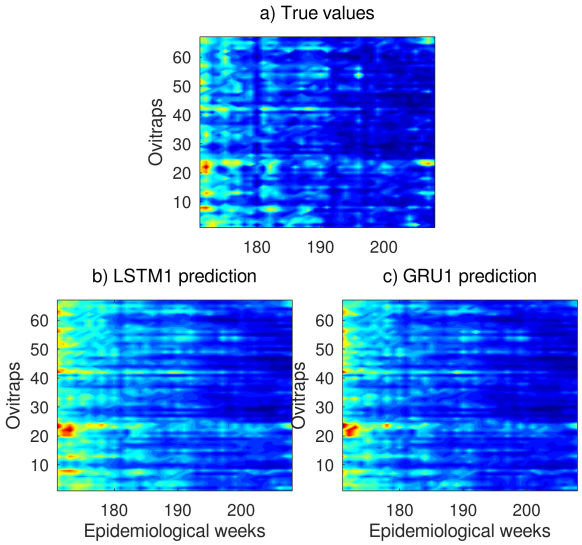

Fig. 6. Performance comparison of models based on the EDI heat maps. (a) Heat map of EDI true values. (b) Heat map of EDI predicted by LSTM1 model. (c) Heat map of EDI predicted by GRU1 model.

expected that individual ovitraps may deviate from the overall mean.

However, it is noteworthy that the models successfully captured the overall trends in individual ovitrap dynamics within the test dataset. Despite the limitations mentioned, the methodology proposed in this study still holds practical relevance for public health interventions. Nonetheless, further improvements are necessary to achieve more accurate predictions for individual spatial ovitraps.

1) Hypothesis test for model comparinson: To assess the statistical significance of the model performance, a hypothesis test was conducted. Given the dependent nature of the samples,

we employed the Wilcoxon signed-rank non-parametric test [11] to compare the performance of the LSTM1 and GRU1 models. This statistical test allowed us to determine whether there was a statistically significant difference in performance between the models. The results revealed that the errors of the models were indeed different, with the LSTM1 model demonstrating slightly superior performance compared to the GRU1 model, and this difference was found to be statistically significant (p-value = 3.64×10^{-12}).

Based on the obtained results and in comparison with the findings presented in Table I, it is noteworthy that the hypothesis test indicated a statistically significant difference in performance between the LSTM1 and GRU1 models. While the validation dataset initially showed lower error rates for the GRU1 model, the test dataset demonstrated that the LSTM1 model achieved slightly lower errors, and this difference was found to be statistically significant. Therefore, both the hypothesis test and the analysis of the test dataset suggest that the LSTM1 model exhibited slightly superior generalization compared to the GRU1 model, with a statistically significant advantage.

V. Final Remarks

The findings of our study emphasize the significance of utilizing ovitrap data to gain insights into the dynamics of arbovirus vectors. The heatmap representation effectively captures the seasonal patterns of the vector population, revealing distinct peaks and valleys. Notably, we observed a strong correlation between ovitrap data and precipitation, highlighting the need for targeted public health interventions during rainy periods.

Among the evaluated machine learning (ML) models, the recurrent models, specifically Long Short-Term Memory (LSTM) followed by Gated Recurrent Unit (GRU), demonstrated superior performance with consistently low error rates. These models generated accurate predictions with minimal deviations from the actual values. The effective capture of temporal dependencies by recurrent deep learning (DL) models, combined with the application of spatial smoothing techniques to reduce randomness and noise, contributed to their exceptional predictive accuracy.

The accuracy achieved by the recurrent DL models further validates their utility as reliable tools for monitoring and preventing arbovirus outbreaks. Their ability to forecast the egg density index trends at fine-grained spatial resolutions aligns well with the requirements for targeted zoonosis interventions. Additionally, the spatial smoothing approach proved effective in reducing randomness and noise, thereby enhancing the precision of the predictions.

These findings hold significant implications for public health interventions. Accurate forecasting of arbovirus vector populations with low errors enables proactive and timely measures to be implemented during periods of heightened risk. By directing resources and interventions to specific locations based on the identified spatial trends, public health efforts can be optimized for effective arbovirus surveillance and prevention.

In terms of future research directions, we aim to utilize updated datasets and incorporate additional climatic variables as predictors. Such enhancements are projected to improve both the accuracy and robustness of our forecasting models, offering a significant contribution to more effective arbovirus monitoring and preventive measures. A pivotal focus for subsequent studies will be the refinement of prediction accuracy, particularly for fine-grained spatial regions. Additionally, we plan to delve into and integrate other state-of-the-art DL methods for time series forecasting, like those highlighted in [12], which will further enrich the methodologies presented in this paper.

In summary, our study highlights the significance of achieving low prediction errors in forecasting arbovirus vector populations using recurrent DL models. The successful combination of spatial smoothing and aggregation techniques, along with the incorporation of temporal dependencies, underscores their potential as valuable tools in public health interventions targeting Aedes aegypti control. These findings contribute to the growing body of knowledge aimed at improving arbovirus surveillance and prevention efforts.

References

[1] P. Kotsakiozi, A. Gloria-Soria, A. Caccone, B. Evans, R. Schama, A. J. Martins, and J. R. Powell, "Tracking the return of aedes aegypti to brazil, the major vector of the dengue, chikungunya and zika viruses," *PLoS Negl. Trop. Dis.*, vol. 11, no. 7, p. e0005653, Jul. 2017.

[2] M. U. G. Kraemer, R. C. Reiner, Jr, O. J. Brady, J. P. Messina, M. Gilbert, D. M. Pigott, D. Yi, K. Johnson, L. Earl, L. B. Marczak, S. Shirude, N. Davis Weaver, D. Bisanzio, T. A. Perkins, S. Lai, X. Lu, P. Jones, G. E. Coelho, R. G. Carvalho, W. Van Bortel, C. Marsboom, G. Hendrickx, F. Schaffner, C. G. Moore, H. H. Nax, L. Bengtsson, E. Wetter, A. J. Tatem, J. S. Brownstein, D. L. Smith, L. Lambrechts, S. Cauchemez, C. Linard, N. R. Faria, O. G. Pybus, T. W. Scott, Q. Liu, H. Yu, G. R. W. Wint, S. I. Hay, and N. Golding, "Past and future spread of the arbovirus vectors aedes aegypti and aedes albopictus," *Nat. Microbiol.*, vol. 4, no. 5, pp. 854–863, May 2019.

[3] J. V. Oliveira Noleto, H. L. Moura do Nascimento Moraes, T. De Moura Lima, J. G. Mendes Rodrigues, D. Tavares Cardoso, K. Chaves Lima, R. Soares de Souza Melo, and G. S. Miranda, "Use of ovitraps for the seasonal and spatial monitoring of aedes spp. in an area endemic for arboviruses in northeast brazil," *J. Infect. Dev. Ctries.*, vol. 14, no. 4, pp. 387–393, Apr. 2020.

[4] H. I. Sasmita, K.-B. Neoh, S. Yusmalinar, T. Anggraeni, N.-T. Chang, L.-J. Bong, R. E. Putra, A. Sebayang, C. N. Silalahi, I. Ahmad, and W.-C. Tu, "Ovitrap surveillance of dengue vector mosquitoes in bandung city, west java province, indonesia," *PLoS Negl. Trop. Dis.*, vol. 15, no. 10, p. e0009896, Oct. 2021.

[5] I. Sanchez-Gendriz, G. F. de Souza, I. G. M. de Andrade, A. D. D. Neto, A. de Medeiros Tavares, D. M. S. Barros, A. H. F. de Morais, L. J. Galvão-Lima, and R. A. de Medeiros Valentim, "Data-driven computational intelligence applied to dengue outbreak forecasting: a case study at the scale of the city of natal, RN-Brazil," *Sci. Rep.*, vol. 12, no. 1, p. 6550, Apr. 2022.

[6] C. T. Codeço, A. W. S. Lima, S. C. Araújo, J. B. P. Lima, R. Maciel-de Freitas, N. A. Honório, A. K. R. Galardo, I. A. Braga, G. E. Coelho, and D. Valle, "Surveillance of aedes aegypti: comparison of house index with four alternative traps," *PLoS Negl. Trop. Dis.*, vol. 9, no. 2, p. e0003475, Feb. 2015.

[7] N. Talkhi, N. Akhavan Fatemi, Z. Ataei, and M. Jabbari Nooghabi, "Modeling and forecasting number of confirmed and death caused COVID-19 in IRAN: A comparison of time series forecasting methods," *Biomed. Signal Process. Control*, vol. 66, no. 102494, p. 102494, Apr. 2021.

[8] K. E. ArunKumar, D. V. Kalaga, C. Mohan Sai Kumar, M. Kawaji, and T. M. Brenza, "Comparative analysis of gated recurrent units (GRU), long Short-Term memory (LSTM) cells, autoregressive integrated moving average (ARIMA), seasonal autoregressive integrated moving average (SARIMA) for forecasting COVID-19 trends," *Alex. Eng. J.*, vol. 61, no. 10, pp. 7585–7603, Oct. 2022.

[9] D. Berrar, "Cross-Validation," in *Encyclopedia of Bioinformatics and Computational Biology*. Elsevier, 2019, pp. 542–545.

[10] T. O. Hodson, "Root-mean-square error (RMSE) or mean absolute error (MAE): when to use them or not," *Geosci. Model Dev.*, vol. 15, no. 14, pp. 5481–5487, Jul. 2022.

[11] S. W. Scheff, "Nonparametric statistics," in *Fundamental Statistical Principles for the Neurobiologist*. Elsevier, 2016, pp. 157–182.

[12] I. Oguiza, "tsai - a state-of-the-art deep learning library for time series and sequential data," Github, 2022. [Online]. Available: https://github.com/timeseriesAI/tsai